Temporal dynamics of neural tuning to kinematics in primary motor cortex during reach-grasp-manipulation.

497.02/GG29

Adam G. Rouse[1,2,3,6], Robert A. Jacobs[4,5,6], Marc H. Schieber[1,2,3,6]
Departments of Neuroscience[1], Neurology[2], Biomedical Engineering[3], Brain & Cognitive Science[4], Computer Science[5], Center for Visual Science[6]
The Del Monte Institute for Neuroscience
University of Rochester, Rochester, NY

Finger Movement Laboratory

Neural Control of Reaching & Grasping

In reach-to-grasp movements, reaching with the arm and grasping with the hand typically are thought to proceed concurrently. We recently found that when subjects reach to different locations to grasp and manipulate various objects, neural activity evolves over time, being related more to location early and object later. We now examine whether different combinations of linear models are better able to describe neural activity than one fixed, linear model.

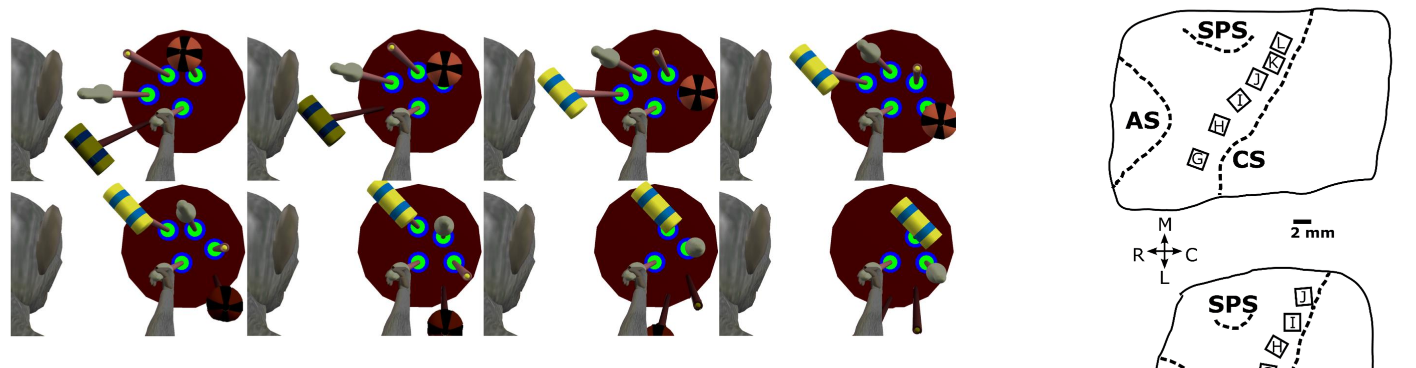

Figure 1. We recorded spiking activity from primary motor cortex (M1) as two monkeys (*Macaca mulatta*), L and X, reached and grasped one of 4 Objects in up to 8 different Locations, then manipulated the object to close a switch.

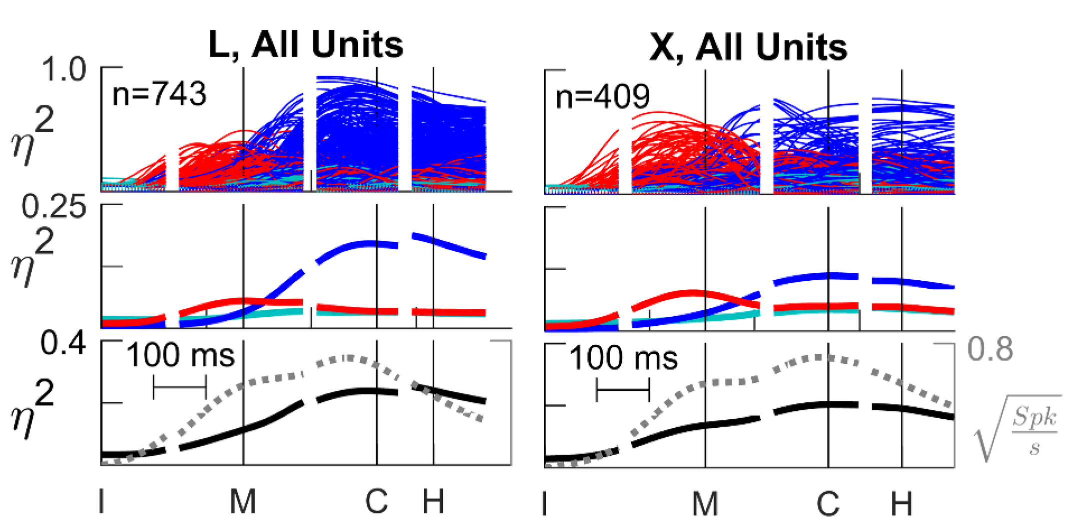

Figure 2. Time resolved ANOVA. The top frame shows overlapped traces of location (red), object (blue), and location x object interaction (cyan) effect size (η2) as a function of time for each unit individually. The middle frame shows mean η2 values across all individual traces from the top frame, averaged separately for location, object, and interaction effects. The bottom frame shows the sum of the three mean η2 values, i.e. the total fraction of variance explained by the task factors (solid black line, left vertical axis), along with the mean change in firing rate from baseline (dashed gray line, right vertical axis).

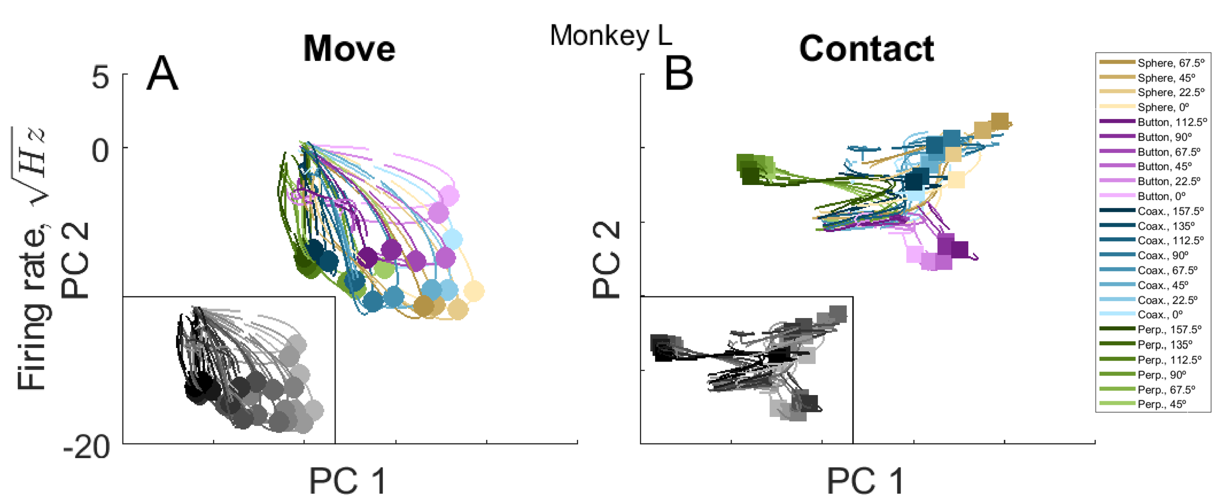

Figure 3. Time-specific principal component analysis for dimensionality reduction in the neural space. PCs were derived from the data at two particular time points: movement onset (left) and peripheral object contact (right). The neural trajectories of the 24 location/object combinations have been projected into the plane of these first two PCs.

- Neuronal activity at the onset of movement was predominantly modulated with Location, while later activity at object contact was predominantly Object-tuned.
- This Location- and Object-related activity occurs in different dimensions as the trajectory of neural activity proceeds through the neural space.

Rouse AG, Schieber MH. (2015). Spatiotemporal distribution of location and object effects in reach-to-grasp kinematics. J of Neurophys. 114(6):3268-82.
Rouse AG, Schieber MH. (2016). Spatiotemporal distribution of location and object effects in primary motor cortex neurons during reach-to-grasp. J of Neurosci. 36(41):10640-10653.

Methods

- 12 kinematic features: the position and velocity of i) x/y/z of the wrist and ii) PC 1-3 of 13 wrist and digit joint angles
- Models predict instantaneous firing rate from kinematics
- Fixed lag of 100 ms with firing rate leading kinematics
- Data sampled at 20 equally spaced time points per trial from onset of movement to peripheral object contact (Median movement time = 255 ms for Monkey L and 235 ms for Monkey X)
- All R^2 values calculated with 10-fold cross-validation

Linear Model

Global Linear Model

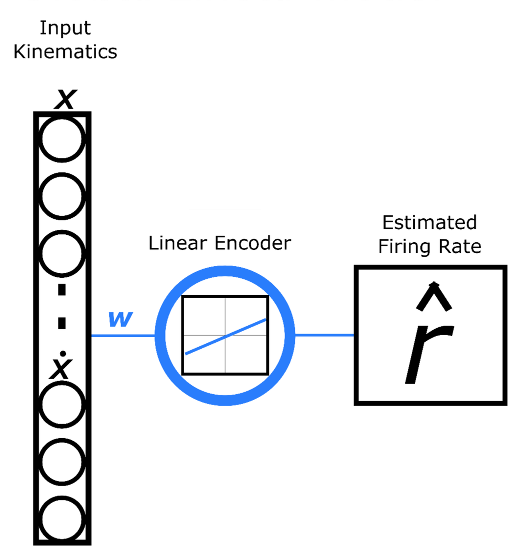

Time-Specific Linear Model

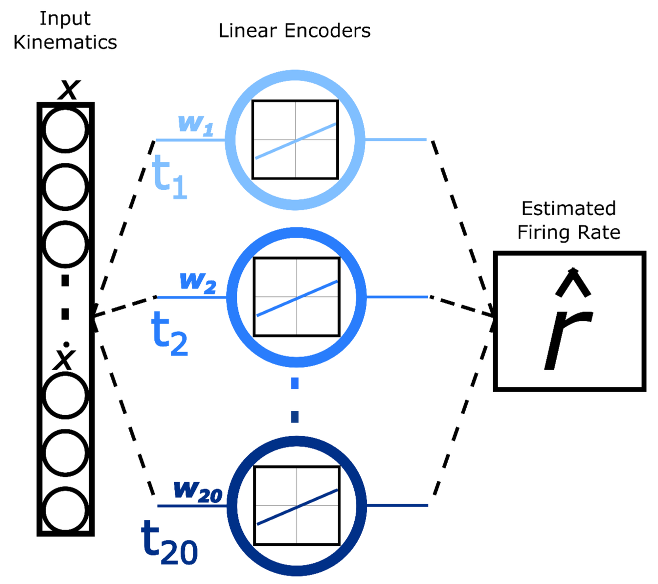

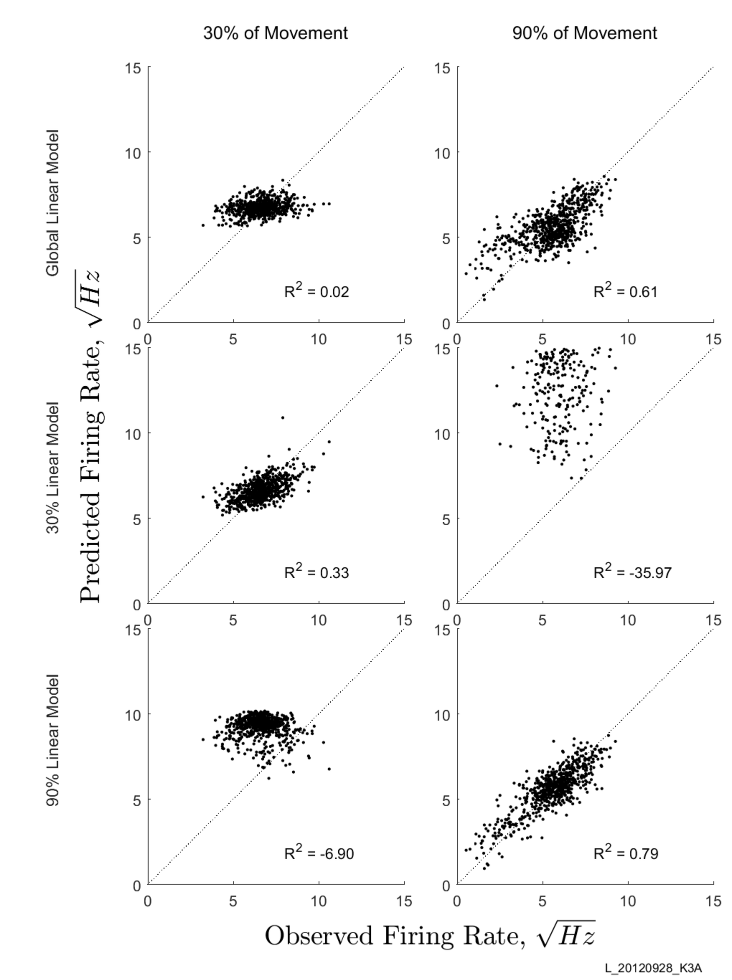

Figure 4. Observed firing rate vs. Predicted firing rate for a global linear model (top row) and two time-specific models: model for t = 30% (middle row) and t = 90% (bottom row) of movement. The model performance is shown at two time points: t = 30% (left column) and t = 90% (right column) of movement.

Mixture of Linear Regression Models

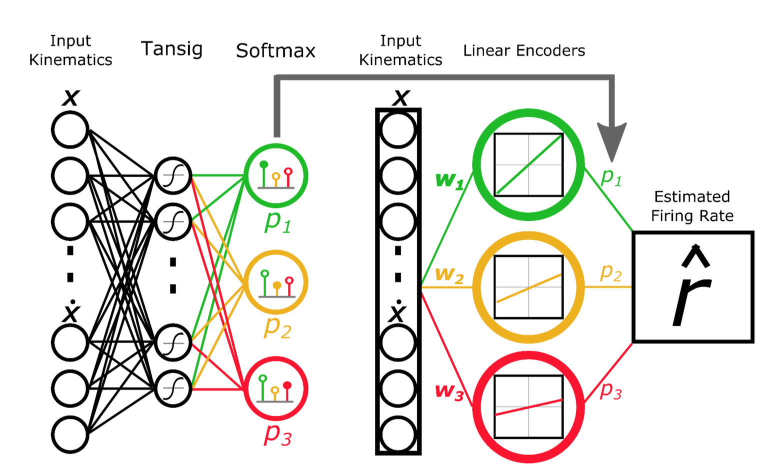

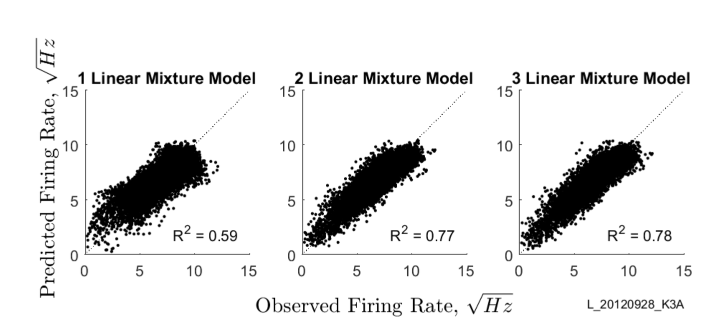

Figure 6. Observed firing rate vs. Predicted firing rate for a mixture of 1, 2, and 3 linear regression models for an example unit.

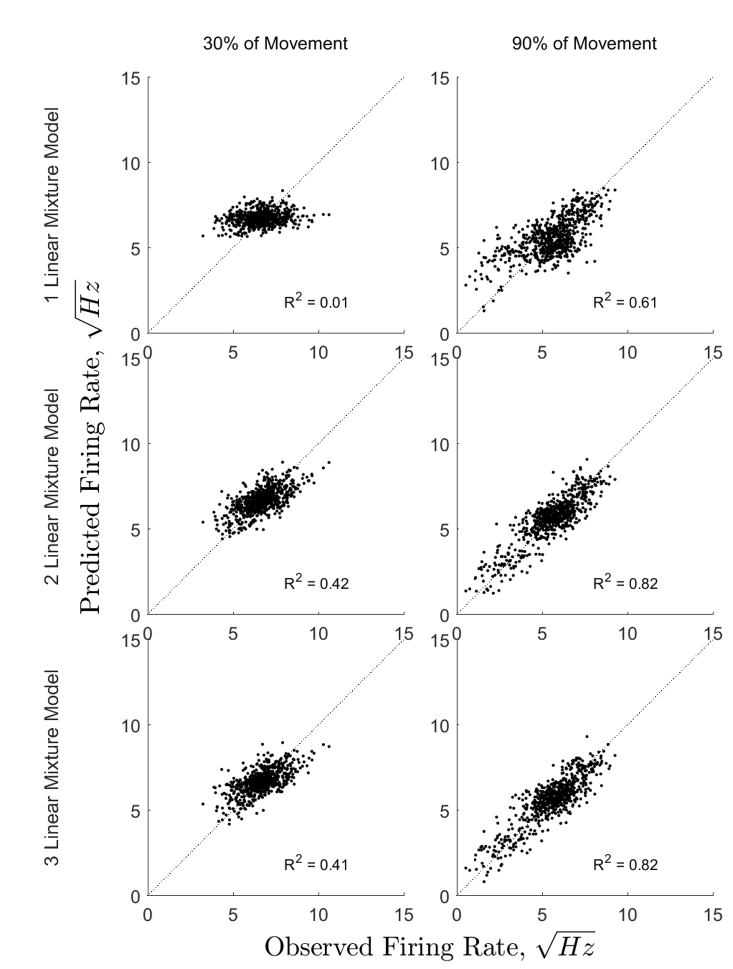

Figure 5. Observed firing rate vs. Predicted firing rate for a mixture of 1 (top row), 2 (middle row), and 3 bottom row) linear regression models. The model performance is shown at two time points: t = 30% (left column) and t = 90% (right column) of movement.

Results

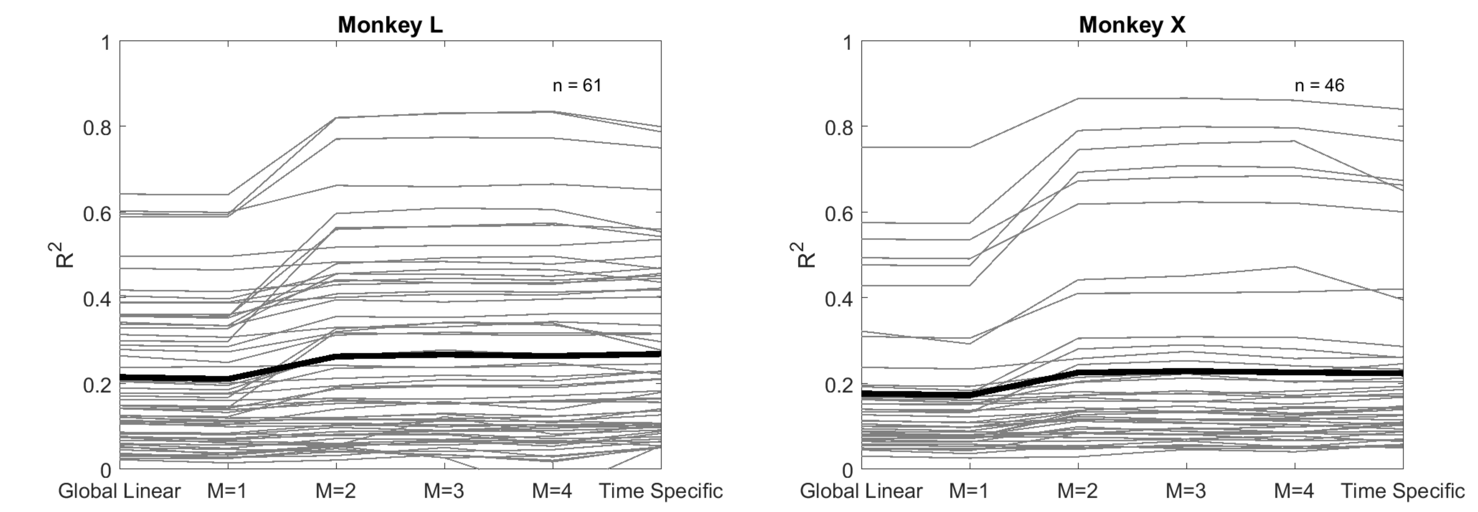

Figure 7. R^2 for individual units. The R^2 values for six different encoding models are shown. Mixtures of linear regression models with 1-4 mixtures is compared to a global linear model (far left) and 20 time-specific linear models (far right). The thick black line represents the mean across all units for a given monkey. The R^2 for the global linear models are 0.21 & 0.17 which increase to 0.26 & 0.23 (monkeys L & X, respectively) for the mixture of only 2 linear regression models. This 2 mixture model performs as well as either those models with more mixing components or the time-specific model.

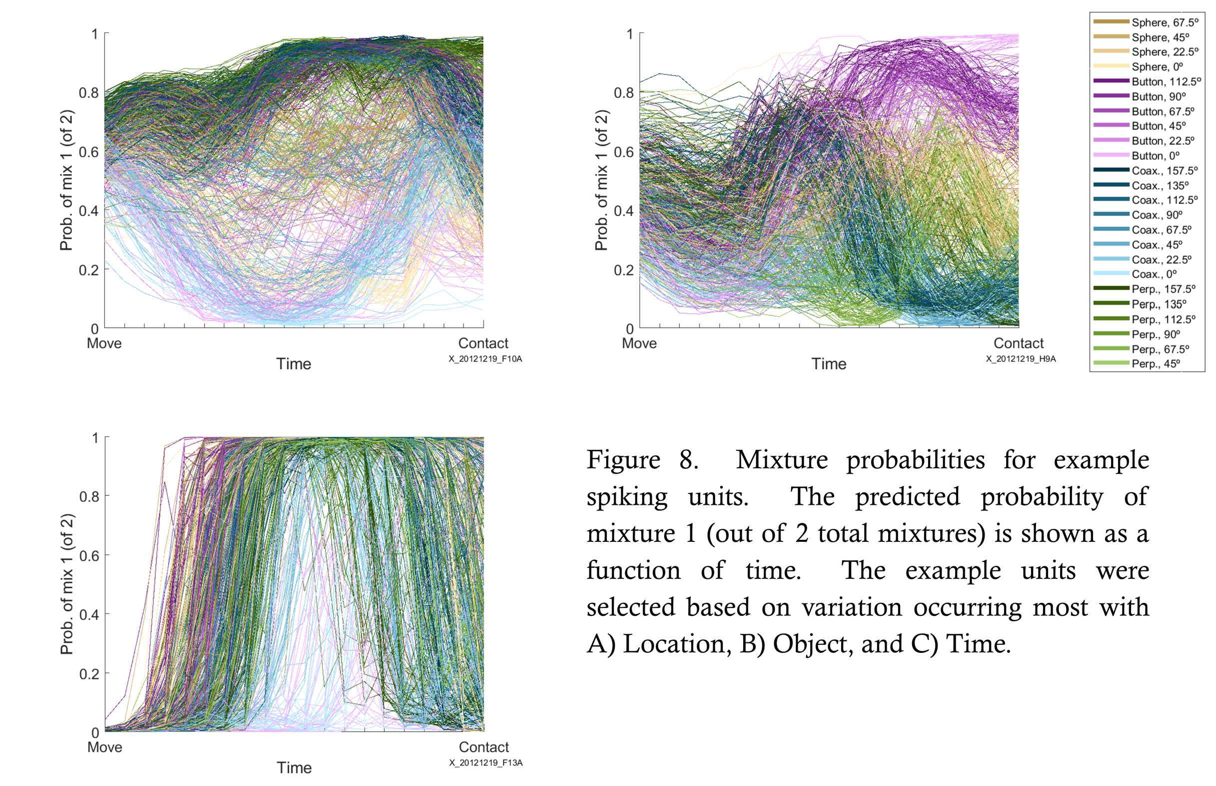

Figure 8. Mixture probabilities for example spiking units. The predicted probability of mixture 1 (out of 2 total mixtures) is shown as a function of time. The example units were selected based on variation occurring most with A) Location, B) Object, and C) Time.

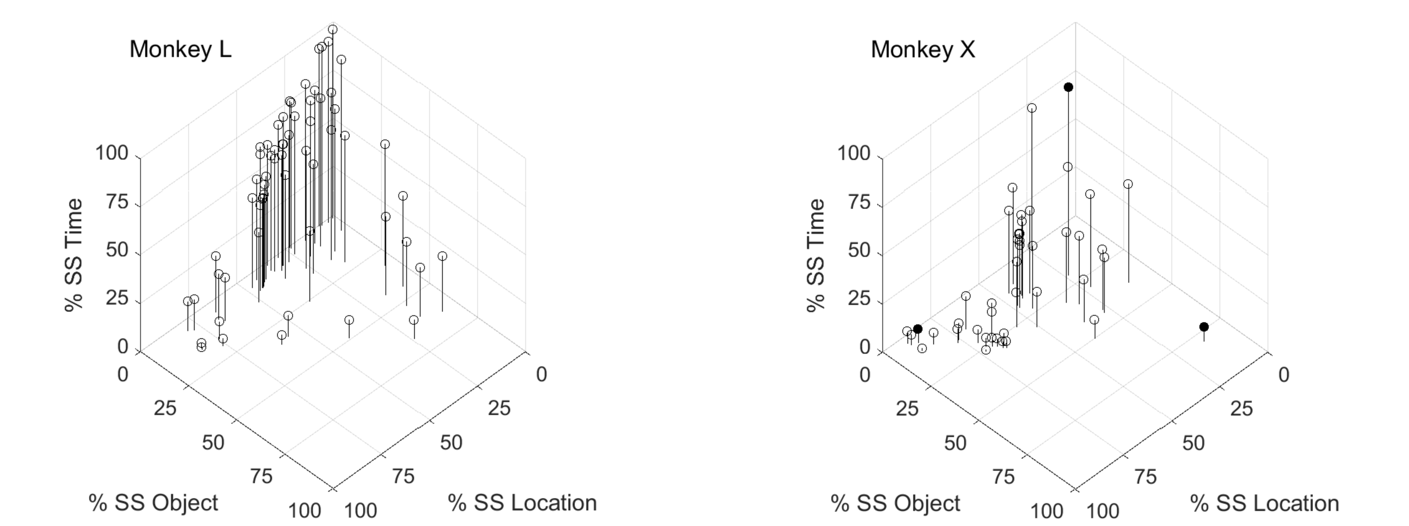

Figure 9. Three-way ANOVA was performed on the probability states of the artificial neural network to determine the effect size related to Location, Object, and Time. The scatter plot shows the percentage of the sum of squares attributed to each factor for each spiking unit. The black circles in the plot for monkey X correspond to the three example units in Figure 8.

Conclusions

- A single linear model of neural encoding does a poor job of generalizing across the early and late phases of movement.
- A mixture of only 2 linear models performs as well as a collection of 20 time-specific linear models.
- The 2 mixture model varied considerably by unit with examples observed that varied primarily with either Location, Object, or Time.

Acknowledgments

This work was supported by NINDS R01-NS079664, and K99-NS101127.